[Chem. Pharm. Bull. 30(12)4468—4478(1982)]

Application of Nonlinear Viscoelastic Analysis by the Oscillation Method to Some Pharmaceutical Ointments in the Japanese Pharmacopeia[1)]

MASAO KOBAYASHI,* SHIGEYUKI ISHIKAWA, and MASAYOSHI SAMEJIMA

Products Formation Research Laboratory, Tanabe Seiyaku Co., Ltd., 16-89, Kashima 3-chome, Yodogawa-ku, Osaka 532, Japan

(Received May 6, 1982)

Several kinds of ointments in the Japanese pharmacopeia were tested in an oscillation rheometer and the results were analyzed by the nonlinear method proposed by Onogi. The stress (σ) curve obtained by application of sinusoidal strain ($\gamma=\gamma_0\sin\omega t$) was approximated by a Fourier series, and the first order function (σ_{1st}) was regarded as the linear part.

A nonlinearity parameter D_{nl} was defined as the difference between observed σ and σ_{1st}. D_{nl} showed different ω dependency for each ointment, and seemed to be related to the pattern of the rheogram. Ordinal viscoelastic parameters such as storage modulus (G'), loss modulus (G''), loss tangent (tan δ), and so on were calculated from the 1st function. The ω dependencies of these parameters were also different for each ointment.

The influence of the weight fraction of solid (f_s) or liquid component ($1-f_s$) on these parameters was examined for simple ointment and macrogol ointment. A bending point was observed on the log G' *vs.* f_s plot, which might correspond to the occurrence of stiff bridge structures in the vehicles. Tan δ of the simple ointment was found to increase, in spite of the increase of solid component. This was presumed to be due to a greater increase of G'' than of G'. This example shows that the increase of f_s does not always result in a relative increase of rheological elasticity.

Continuous shear measurement was performed with a Ferranti-Shirley viscometer and several parameters were compared with those obtained by the oscillation method. The correlation seemed to be closer when the shear rate was smaller.

Keywords——white ointment; simple ointment; hydrophilic vaseline; macrogol ointment; nonlinear viscoelastic analysis; oscillation method; storage modulus; loss modulus; degree of nonlinearity

The rheological properties of semisolid ointments and creams are regarded as influencing their physical stability,[2)] sensory evaluation,[3)] percutaneous absorption of active ingredients, manufacturability,[4)] and many other important phenomena. Various instruments (penetrometer, spreadmeter, rotational viscometer) and methods (continuous shear method *etc.*) have been used for evaluation, but a rather high shear rate is usually necessary, and consequently the physical structures of samples are considered to be destroyed in the measuring procedure. Therefore, the rheological values obtained by these methods for most semisolids are those during or after the destruction of physical structures. Thus, different values are often observed for even the same preparations depending on the measuring methods, the apparatus, the history of applied shear rate, the history of storage temperature, and so on. This complexity may be one of the causes of the problems often found in correlating rheological properties with practical phenomena during the development or manufacture of semisolid pharmaceuticals.

Therefore, Barry *et al.* recommended measurement of the rheological properties at the rheological ground state where the testing method does not significantly alter the physical structure.[5)] Indeed, some properties, such as the release of active ingredients from the vehicle, bleeding of liquid components from the vehicle, the floatation or sedimentation of particles in emulsion preparations, the formation of liquid crystals, and so on, are intuitively presumed to have a closer correlation with the static state than the structurally destroyed state of vehicles.

Thus, they frequently adopted a creep or oscillation test because the shear rates of these methods are much smaller than those of other conventional methods.[2]

However, even in these methods, another troublesome problem, nonlinearity, should be taken into consideration. Therefore, Barry or Davis restricted the measuring shear strain to the region where linearity held good.[6] However, this seems to narrow the applicability of these methods because expensive instruments are necessary and the linearity check is troublesome.[7]

Onogi *et al.* presented a theoretical analysis of rheological nonlinearity in the oscillation method and applied it to some suspensions and emulsions.[8] Their method seemed useful for the evaluation of some pharmaceutical semisolids. Thus we examined whether their method was applicable to some typical ointments in the Japanese pharmacopeia (JP) such as white ointment (WO), simple ointment (SO), hydrophilic vaseline (HV) and macrogol ointment (MGO), and calculated ordinal viscoelastic parameters such as storage modulus (=dynamic modulus) (G'), loss mudulus (G''), dynamic viscosity (η'), and loss tangent (tan δ) from the linear region. At the same time, as the nonlinearity itself seemed to reflect some physical features of the vehicles, we defined the degree of nonlinearity, D_{nl}, and calculated it for each ointment. The possible physical significance of these linear and nonlinear parameters is discussed in terms of their dependency on ω or on the raw material composition.

Theoretical

The stress (σ) of a perfect elastic solid is always directly proportional to strain (γ) but independent of the rate of strain ($\dot{\gamma}=d\gamma/dt$), whereas that of a Newtonian liquid is directly proportional to $\dot{\gamma}$ but independent of γ itself. However, the stress of semisolids usually depends on both γ and $\dot{\gamma}$, namely the materials show viscoelastic behavior. In this case, if the ratio of σ to γ is a function of time alone, then the material is regarded as linearly viscoelastic, whereas if it is a function of both the stress magnitude and time, then the relationship is regarded as nonlinear.[5]

In the oscillation method, the strain is applied sinusoidally, $\gamma(t)=\gamma_0 \sin \omega t$, where γ_0 and ω are the amplitude and frequency, respectively. If the material shows linear behavior, then σ also shows a sinusoidal pattern, $\sigma(t)=\sigma_0 \sin(\omega t+\delta)$, where σ_0 and δ are a constant and the difference of phase, respectively. Therefore the resulting curves of σ—γ on X—Y plotting should display a perfect ellipse known as the Lissajou ellipse.

The viscoelastic parameters such as G', G'', η' can be calculated from the Markovitz equation for linear materials,[9] but in nonlinear cases, $\sigma(t)$ deviates from the sinusoidal curve and this equation cannot be applied. Onogi *et al.* derived the following equation for nonlinear $\sigma(t)$

$$\sigma(t) = (G_{11}'\gamma_0+G_{13}'\gamma_0^3)\sin\omega t + (G_{11}''\gamma_0+G_{13}''\gamma_0^3)\cos\omega t - G_{33}'\gamma_0^3\sin 3\omega t - G_{33}''\gamma_0^3\cos 3\omega t + \ldots \quad (1)$$

where G_{11}', G_{11}'', *etc.* are related to the after-effect functions.[8]

If the cone-and-plate type viscometer is used, then

$$M(t) = (2/3)\pi R^3\sigma(t) \quad (2)$$

where $M(t)$ is the torque and R is the radius of the cone-and-plate. If $M(t)$ can be expressed approximately by a Fourier series, then

$$M(t) = K\sum(a_n \sin n\omega t + b_n \cos n\omega t) \quad (3)$$

where K and a_n and b_n are the torsion constant and the amplitudes of constituent waves. When a_n and b_n are negligibly small for even n, then

$$
\begin{aligned}
G_1' &= G_{11}' + G_{13}'\gamma_0^2 = (3Ka_1/2\pi R^3)(\varepsilon/\lambda) \\
G_1'' &= G_{11}'' + G_{13}''\gamma_0^2 = (3Kb_1/2\pi R^3)(\varepsilon/\lambda) \\
G_3' &= G_{33}' = -(3Ka_3/2\pi R^3)(\varepsilon/\lambda)^3 \\
G_3'' &= G_{33}'' = -(3Kb_3/2\pi R^3)(\varepsilon/\lambda)^3
\end{aligned} \tag{4}
$$

where λ and ε are the amplitude of the input sine wave and the cone angle, respectively. The strain amplitude can be expressed as $\gamma_0=(\varepsilon/\lambda)$.

When γ_0 is small enough, G_1' and G_1'' can be regarded as the parameters of the linear part of σ, while G_3', G_3'', *etc.* can be regarded as parameters of nonlinear parts.[8]

Experimental

Materials——Four kind of ointments, MGO, SO, HV, and WO were prepared after the formulae described in JP X. The ingredients were mixed in a mixer (T.K Agihomomixer HV-M, Tokushu Kika Kogyo Co., Ltd.) at 80°C for about 15 min with the homomixer set at 5000 rpm and the paddle mixer at 30 rpm. Then they were cooled to about 55°C for 30 min and the homomixer was stopped. The cooling was continued to room temperature with mixing by the paddle mixer for about 1 h. The ointments obtained were allowed to stand at 25°C for more than a week to attain rheological equilibrium before the measurements. Vaseline (VAS) and lanolin (LN) were examined as representative raw materials and were treated similarly to the ointments.

The materials used to prepare these ointments were as follows: VAS, LN, beeswax (BW), soybean oil, Macrogol 400, Macrogol 4000, cholesterol (CS) and stearyl alcohol (SA). These materials were obtained from commercial sources and satisfied the requirements of JP X.[10]

Rheological Measurement——1) Oscillation Method: A Shimadzu RM-1 rheometer fitted with a cone-and-plate system was used. The temperature at the measurement unit was controlled at 25 ± 0.1°C by the circulation of thermostated water. Measurement conditions were as follows: frequency (ω), 2×10^{-3}—4.7×10^{-1} (rad/s); cone angle (ε), 7×10^{-2} (rad); strain amplitude (λ), 1.75×10^{-2} (rad); radius of cone-and-plate (R), 1.5 (cm); torsion constant of wire (K), 2.22×10^6, 9.05×10^6 or 2.49×10^7 (dyn·cm/rad). The wire was chosen according to the viscosity of samples.

2) Continuous Shear Method: A Ferranti-Shirley cone-and-plate viscometer was used as follows: sweep time, 1 min; shear rate, 0—625 (s^{-1}). The apparent viscosity (P) at $\dot{\gamma}=120$ s^{-1} (η_{120}) and at $\dot{\gamma}=625$ s^{-1} (η_{625}), and the static yield value (SYV) (dyn/cm^2) were obtained on the up curve as shown in Fig. 1.[11]

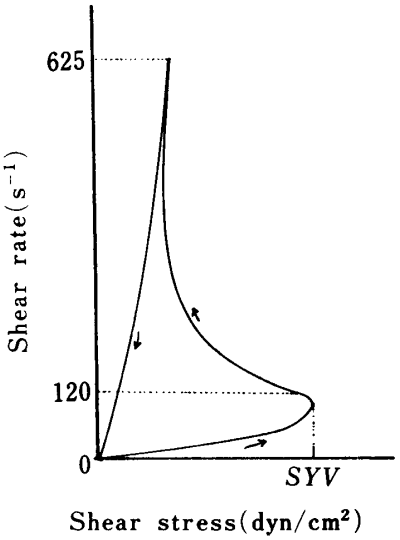

Fig. 1. Typical Flow Curve obtained using the Ferranti-Shirley Cone-and-Plate Viscometer

Computation Method——The signals of the stress were amplified and drawn on the recorder. The distance, I (cm), from the center of the stress curve was read at 36 equal intervals in one cycle (0—2π). Then, multiplying I by the amplifying constant of the recorder (f) (rad/cm), the torsion angle I' (rad) could be obtained. Here, $I'(t)$ corresponds to $M(t)/K$ in Eq. (3). The regression of $I'(t)$ to a Fourier series was performed and the coefficients a_n and b_n were obtained by use of the MATH PAC program (Hewlett Packard).

For example, in the case of WO at $\omega=0.0116$ (rad/s), a_1 and b_1 were calculated as 5.51×10^{-4} (rad) and 8.25×10^{-4} (rad) respectively, then G_1' and G_1'' are obtained as 2.81×10^3 (dyn/cm^2) and 4.20×10^3 (dyn/cm^2), respectively, according to Eq. (4) with the apparatus constant described above. The torsion constant K was 9.05×10^6 (dyn·cm/rad) in this case.

Results and Discussion

Examination of the Applicability of Nonlinear Analysis

Onogi indicated that the following premises are necessary for their method to be applicable, namely, 1) the stress waves should be approximated by a Fourier expansion without very high harmonics and 2) the amplitude of the even harmonics should be negligibly small

as compared with those of the odd harmonics. Therefore, we defined the extent of the deviation (D_{ev}) between the calculated wave ($\sigma_{cal.}$) and the observed ones ($\sigma_{obs.}$) by equation (5), and examined whether the two premises were realized.

$$D_{ev} = \left(\int_0^{2\pi} |\sigma_{obs.} - \sigma_{cal.}| d\theta\right) \Big/ \left(\int_0^{2\pi} |\sigma_{obs.}| d\theta\right) \tag{5}$$

where θ is expressed as $\theta = \omega t$. The values of $\sigma_{cal.}$ were estimated by using Eq. (2), (3), and each a_n and b_n value obtained as described above.

$$\begin{aligned} \sigma_{cal.,\ n=1} &= (a_1 \sin\theta + b_1\cos\theta) \times 3K/2\pi R^3 \\ \sigma_{cal.,\ n=2} &= \sigma_{cal.,\ n=1} + (a_2\sin 2\theta + b_2\cos 2\theta) \times 3K/2\pi R^3 \\ \sigma_{cal.,\ n=3} &= \sigma_{cal.,\ n=2} + (a_3\sin 3\theta + b_3\cos 3\theta) \times 3K/2\pi R^3 \end{aligned} \tag{6}$$

Consequently, all the σ curves were found to satisfy the permises and their method could therefore be applied. Table I shows, as examples, the calculated a_n and b_n values, and how the D_{ev} values were improved for WO and MGO at $\omega = 0.0116$ (rad/s). In these cases, D_{ev} values were large at the first approximation (23% for WO and 16% for MGO), and decreased with odd n numbers but seldom changed with even n. It was also found that D_{ev} was reduced to within a few percent with 5th order approximation. In Fig. 2a, the calculated wave ($n=5$) and the experimental one for WO are compared as an example. At the same time, the

Table I. The Improvement of D_{ev} Values with Harmonic Number (n)

n	WO					MGO				
	D_{ev}	$a_n \times 10^4$ (rad)	$b_n \times 10^4$ (rad)	$G' \times 10^{-3}$ (dyn/cm²)	$G'' \times 10^{-3}$ (dyn/cm²)	D_{ev}	$a_n \times 10^4$ (rad)	$b_n \times 10^4$ (rad)	$G' \times 10^{-3}$ (dyn/cm²)	$G'' \times 10^{-3}$ (dyn/cm²)
1st	.233	5.51	8.25	2.81	4.20	.156	1.07	6.55	0.55	3.34
2nd	.233	−0.17	0.24			.156	−0.02	−0.03		
3rd	.059	−1.95	−1.14	8.92	5.23	.065	−0.65	−0.71	2.97	3.27
4th	.059	−0.02	−0.04			.065	0.04	0.03		
5th	.018	0.48	0.31	247.0	158.0	.035	0.35	0.13	183.0	66.7

$\omega = 0.0116$ (rad/s), $K = 9.05 \times 10^6$ (dyn·cm/rad).

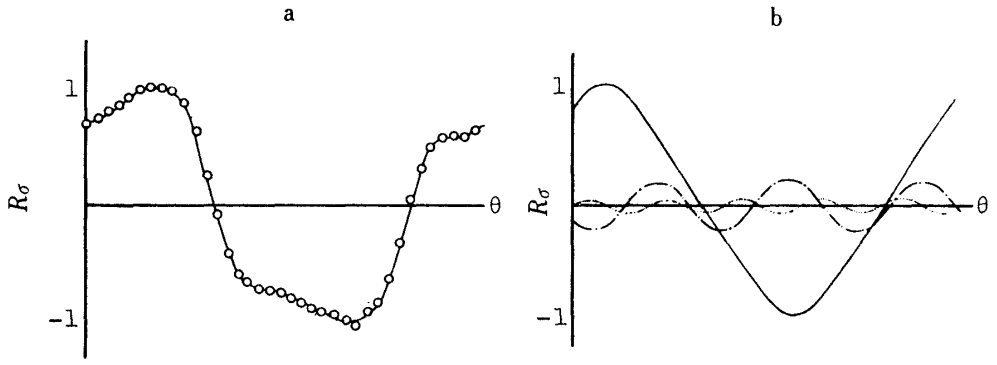

Fig. 2. An Example of the Relation between the Observed and Calculated σ Values

Ointment, WO; $\omega = 0.0116$ (rad/s); strain $\gamma = \gamma_0 \sin\omega t$.
(a) Open circles are observed δ values and the line is the approximating function, $R\sigma_A$. (b) The 1st ($R\sigma_1$,—), the 3rd ($R\sigma_3$, -·-), and the 5th ($R\sigma_5$ ···) wave functions are shown. $R\delta$ means σ/σ_{max} and is the same as I'/I'_{max}. The functions are as follows: $R\sigma_1 = (a_1 \sin\theta + b_1\cos\theta)/I'_{max}$, $R\sigma_3 = (a_3\sin 3\theta + b_3\cos 3\theta)/I'_{max}$, $R\sigma_5 = (a_5\sin 5\theta + b_5\cos 5\theta)/I'_{max}$, $R\sigma_A = R\sigma_1 + R\sigma_3 + R\sigma_5$. Here, I'_{max} means the maximum value of observed I' and is 8.95×10^{-4} (rad). The values of a_n and b_n are shown in Table I.

1st, 3rd, and 5th waves are shown in Fig. 2b; the amplitude of the 1st wave was overwhelmingly larger than that of the 3rd or 5th one.

The Degree of Nonlinearity

G_1' and G_1'' can be regarded as the storage modulus and loss modulus of the linear part, respectively, whereas G_3', G_3'', ..are the parameters expressing the nonlinear parts.[8] These values were calculated for the above two ointments as examples (Table I). These nonlinear parameters were large in spite of the smaller amplitude of the nonlinear function. Thus, the physical significance of these nonlinear parameters is rather unclear.

Kotaka *et al.* used $[(G_j'^2+G_j''^2)/(G_1'^2+G_1''^2)]$ $(j=3,5)$ as nonlinear parameters,[12] but these also seem to be of uncertain physical significance. Therefore we defined the nonlinearity parameter in this paper as

$$D_{n1} = \left(\int_0^{2\pi} |\sigma_{obs.} - \sigma_{1st}| d\theta\right) \Big/ \left(\int_0^{2\pi} |\sigma_{obs.}| d\theta\right)$$

where σ_{1st} is σ of the 1st approximation and has the same meaning as $\sigma_{cal.,n=1}$ in Eq. (6). This value simply expresses the contribution ratio of total nonlinearity to the stress and seems more understandable. The D_{n1} values of the four ointments and the two raw materials are shown in Fig. 3 together with those of JS-200H, the standard Newtonian liquid, in the ω range from 2×10^{-3} to 4.7×10^{-1} (rad/s) (Fig.3). It was shown that D_{n1} became smaller with increase of ω in the cases of SO, MGO, LN, and VAS. Davis measured the viscoelasticity of several ointments in the linear region, and mentioned that the linearity generally improved with increase of ω.[6c] Thus, these results are in accord with theirs. However, in the cases of HV and WO, D_{n1} had a maximum at $\omega=0.05$ and the linearity was good even at low ω. This was inconsistent with Davis's description. D_{n1} of Newtonian liquid was confirmed to be negligible compared with those of the other vehicles. These results will be discussed later.

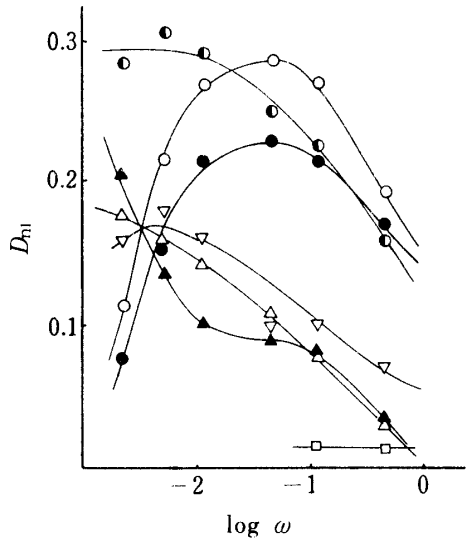

Fig. 3. The ω Dependency of the Nonlinearity Parameter D_{n1} for Various Semisolid Materials at 25°C

Symbols: SO (◐), HV (○), WO (●), MGO (△), VAS (▽), LN (▲), JS-200H (□).

Dynamic Viscoelastic Parameters calculated from the Linear Region

As can be seen from Fig. 3, the nonlinearity of the ointments was 30% at most, so at least 70% of the stress can be regarded as arising from the linear part.

Figure 4 shows G' $(=G_1')$ (dyn/cm^2), η' $(=G_1''/\omega)$ (P), and $\tan\delta(=G_1''/G_1')$ calculated from the 1st wave function. The G' values of SO, WO, and HV did not change much with ω, whereas those of MGO, VAS, and LN increased with ω. The η' values decreased with ω, and this is consistent with the results for many viscoelastic materials. The loss tangent is regarded as an index of the relative contributions of liquidity and solidity to σ. Davis indicated that the pattern of a plot of $\tan\delta$ against ω may be useful for the classification of ointment bases.[6b] Figure 4c suggests that the patterns of $\tan\delta$ of the six vehicles can be classified into 3 groups, that is, 1) decreased rapidly with ω (MGO and LN), 2) scarcely changed with ω (WO and HV), and 3) reached a maximum value (SO and VAS).

If the rheological behavior can be understood in terms of a combination of dashpots and springs (Maxwell type model), the dashpots work more effectively at relatively smaller ω,

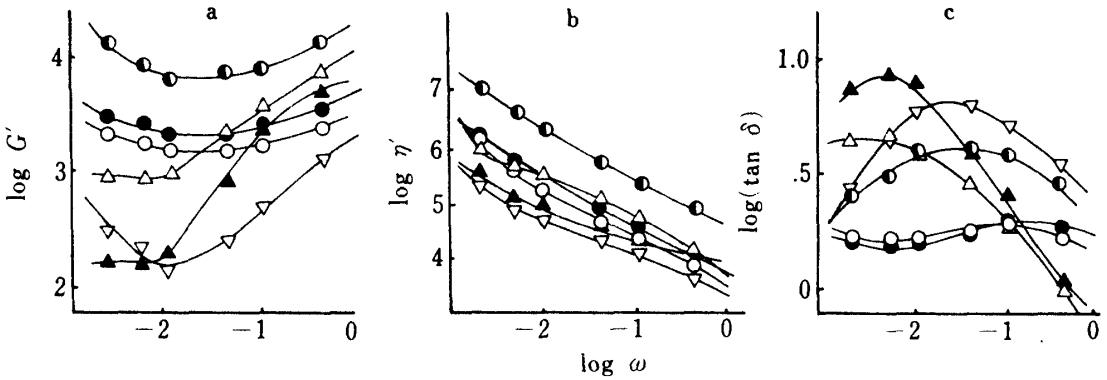

Fig. 4. Viscoelastic Parameters of Various Ointments calculated from the Linear Part of σ

The symbols are the same as in Fig. 3.

whereas the springs work more effectively at rather larger ω. In such a case, tan δ is expected to decrease with ω. The behavior of group 1 was in accord with this expectation. On the other hand, constant tan δ values mean that the G' dependency on ω is almost the same as that of G''. The reason for the existence of the plateau as in group 2 or the maximum values as in group 3 is not clear, but it is interesting that group 2 and group 3 had larger D_{nl} values than group 1.

The Influence of the Composition of Raw Materials

In order to determine the influence of the composition of liquid and solid components, SO and MGO were prepared with various liquid and solid compositions and their properties were measured.

Figure 5 shows G' and D_{nl} of SO having various solid component weight fractions, f_s, defined as follows

$$f_s = W_s/(W_s + W_l) \tag{7}$$

where W_s and W_l mean the weight of solid and liquid in a vehicle, respectively. For SO, the solid component is beeswax and the liquid phase is soybean oil.

It was found that G' displayed similar values and ω dependency when f_s was more than 0.25, but decreased abruptly when f_s was below 0.20. This f_s dependency was similar to that of D_{nl}.

Figure 6 shows the changes of G', tan δ, and D_{nl} for SO against f_s values at ω=0.47 (rad/s). The values for MGO are also plotted. In this case, the solid and liquid components were Macrogol 4000 and 400, respectively.

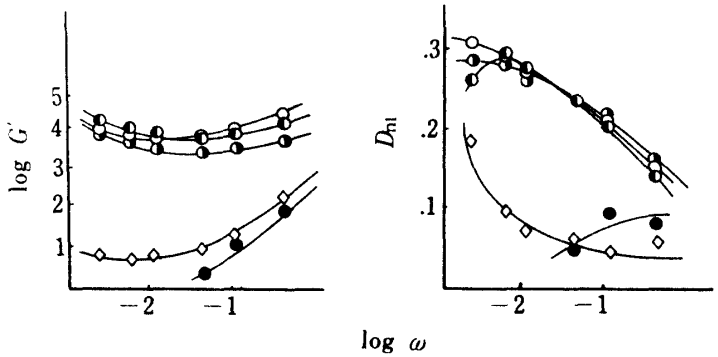

Fig. 5. The Influence of the Composition of Simple Ointment on the Viscoelastic Behavior

The weight fractions of BW were 40% (◐), 33% (◑), 25% (○), 20% (◇), and 10% (●).
Solid component, BW; liquid component, soybean oil.

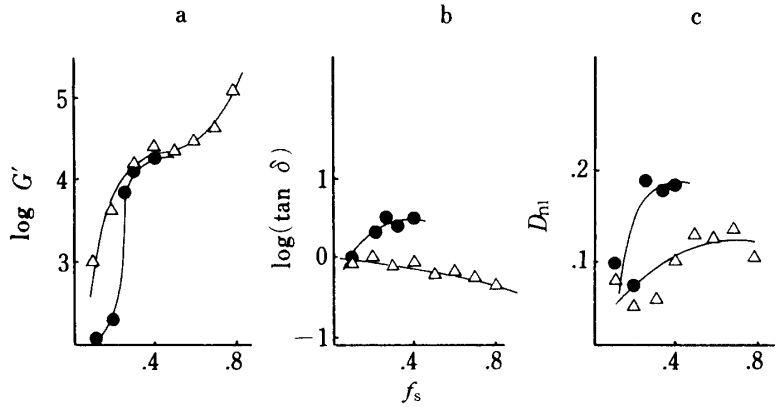

Fig. 6. The Influence of the Weight Fraction of the Solid Component on the Viscoelastic Parameters of SO (●) and MGO (△) at $\omega=0.47$ (rad/s)

MGO and SO both had bending points on the log G' *vs.* f_s plots at about $f_s=0.25$ (Fig. 6a). This was presumed to be caused by the increase in the number of contact sites among solid particles, so that more bridge structures are formed and the vehicles become stiffer. When f_s is less than 0.20, the liquid component can affect the rheological properties by acting as a lubricant, but at f_s above 0.25, the bridge structures may be too stiff for their properties to change much due to a small increase of the solid component. Thus the increase of G' with f_s is presumed to be modest when f_s exceeds the value at the bending point.

The dependency of tan δ on f_s was as expected for MGO, that is, it decreased with f_s. The decrease means that the relative increase of the elasticity (therefore solidity) was more than that of the viscosity (that is liquidity). However, for SO, it increased with f_s. The latter result may be caused by a relatively larger increase of G'' than of G'. These findings mean that the solidity or liquidity assessed rheologically does not always reflect the composition of solid and liquid materials in the vehicle.

The Influence of the Various Raw Materials added to Vaseline

BW, SA, CS, and LN, which are used for the preparation of HV or WO, were added to

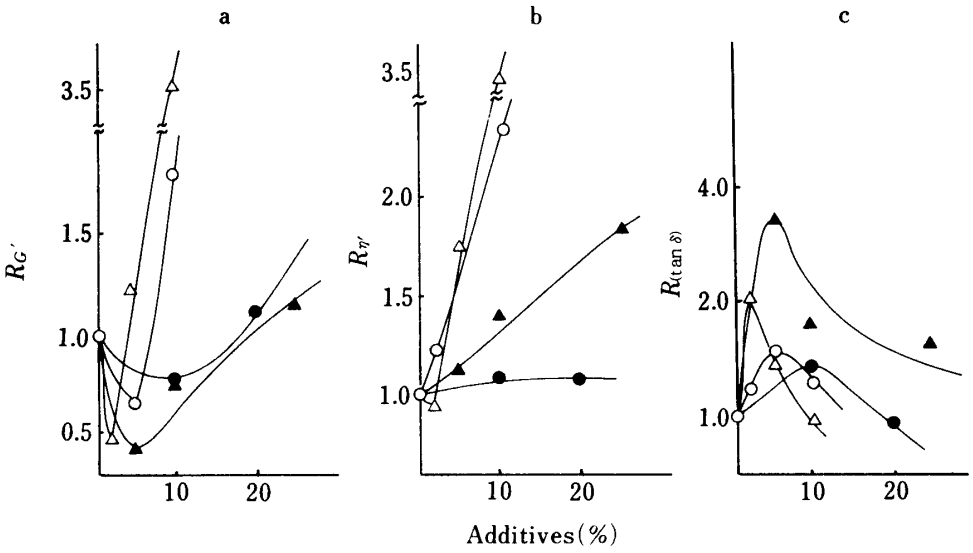

Fig. 7. The Influence of Additives on the Viscoelastic Properties of VAS at $\omega=0.47$ (rad/s)

Additives: LN (▲), BW (○), SA (△), and CS (●).

VAS at various weight fraction ratios and the viscoelastic parameters of the mixtures were measured.

Figure 7 shows the changes of G', G'', and tan δ with the weight fraction of additives. Here, $R_{G'}$, means the ratio of G' of the mixed vehicle to that of VAS alone, that is, $R_{G'}=(G'_{\text{mixed vehicle}}/G'_{\text{vaseline}})$ and $R\eta'$ and $R_{\tan\delta}$ have similar meanings.

It was shown that G' decreased with the addition of these solid additives at first, contrary to expection, then increased after reaching a minimum. For η', scarcely any secrease was observed. The reason for the decrease of G' was not obvious, but possibly the orientation of the native vaseline structure is obstructed by the added materials. However, as the content of stiff materials increases, their properties become predominant in the vehicles, and thus G' increases after reaching a minimum value. The existence of a maximum in $R_{\tan\delta}$ may support this suggestion (Fig. 7c).

Discussion of the Nonlinearity of the Semisolids

Figure 8 shows examples of the σ curves of some ointments whose D_{nl} values were about 0.3, 0.15, and 0.05, respectively. Here, for convenience of comparison, σ was expressed in terms of $R\sigma$, which is defined as $\sigma/\sigma_{\max}$, where $\sigma_{\max}$ is the maximum σ value.

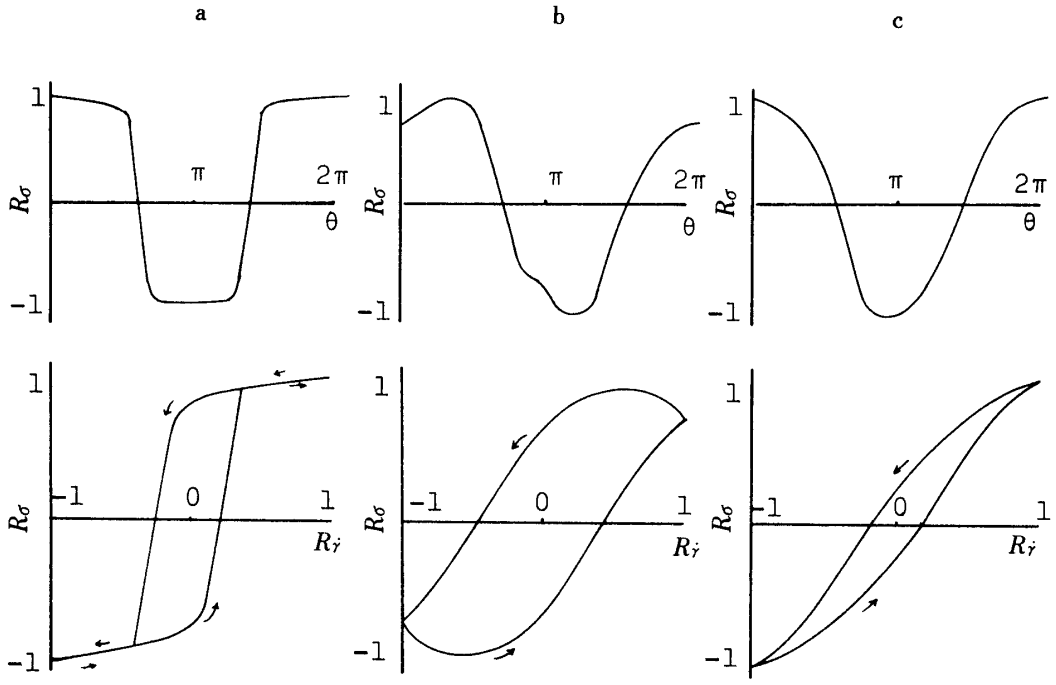

Fig. 8. Typical Patterns of σ-θ and σ-$\dot{\gamma}$ Relations

a, $D_{\text{nl}}=0.3$ (SO); b, $D_{\text{nl}}=0.15$ (WO); c, $D_{\text{nl}}=0.05$ (MGO).
Each measurement was made at $\omega=0.0116$ (rad/s).

The relative shear rate $R_{\dot{\gamma}}$ is also plotted against R_σ in the lower figures, where $\dot{\gamma}$ (rad/s) was calculated as $\dot{\gamma}=d\gamma/dt=d(\gamma_0\sin\omega t)/dt=\omega\gamma_0\cos\omega t$, and hence $R_{\dot{\gamma}}=\gamma/\omega\gamma_0$. Thus, the lower figures show the ordinal rheograms, which express the relationship between shear rate and stress. It is known that the larger the D_{nl} values, the more the R_σ curves deviate from sinusoidal and the greater the yield value. Namely, in the case of $D_{\text{nl}}=0.3$, R_σ scarcely changed at $-1<R_{\dot{\gamma}}<0$, rapidly increased at $0<R_{\dot{\gamma}}<0.3$, and then scarcely changed at $0.3<R_{\dot{\gamma}}<1$. In the down curve of $\dot{\gamma}$, R_σ suddenly decreased at $-0.3<R_{\dot{\gamma}}<0$. In this rheogram, the up and down curves could not be superimposed, and a hysteresis loop was formed. This loop seemed to take the shape of a parallelogram at larger D_{nl} values. As

the D_{nl} values became smaller, the yield value became less and the shape of the hysteresis loop moved away from a parallelogram. The relation between D_{nl} and σ-θ ($\theta=\omega t$) or σ-$\dot{\gamma}$ pattern was common for all other cases. Thus, it seems possible to anticipate σ patterns from the nonlinearity parameter D_{nl}.

Semisolid vehicles can be regarded as gel-like dispersion systems where the structure elements are dispersed in a fluid medium. The rheological behavior of these systems often shows nonlinearity. The causes of this have been discussed by many researchers from the viewpoint of the physical state at the micro level, and change of orientation of the dispersed particles, deformation, shortening, adsorption of dispersed phase on particles, immobilization, and so on, occurring under shear strain, were proposed to be involved.[13]

In view of the fact that a remarkable yield value was observed for the rheogram when D_{nl} was large, immobilization may be one of the main causes of nonlinearity. On the other hand, the well known fact that many kinds of semisolids reduce the viscosity or elasticity to some extent at strong shear strain may reflect the involvement of deformation or shortening of structures. Thus, the nonlinear behavior of the ointments may be attributable to a complex interaction of several of the above phenomena. Thus, D_{nl} values seem to be a convenient parameter to express the extent of the complication of the rheological behavior of the vehicle.

Davis *et al.* reported that nonlinearity was more noticeable at low ω value. This was in accord with our findings for LN, VAS, MGO, and SO (Fig. 3), but not for WO and HV. The reason for the former behavior may be that immobilization occurred more easily because the shear rate was small at small ω, and consequently D_{nl} might take larger values. The reason is not clear in the latter case, but may be related to the raw material composition of the vehicle. As WO and HV contain BW, CS, or SA in VAS, ointments containing 2, 5, or 10% BW, 10 or 20% CS, or 10 or 20% SA in VAS were prepared and their D_{nl} values were measured. The vehicle containing 10% BW or 20% CS showed a pattern having a maximum D_{nl} value. However all other vehicles showed a monotonous decrease, as in the case of 20% SA (Fig. 9). Thus, an increase of solid component such as BW or CS seemed to produce a maximum of D_{nl}. However, further study is necessary to clarify these phenomena in more detail.

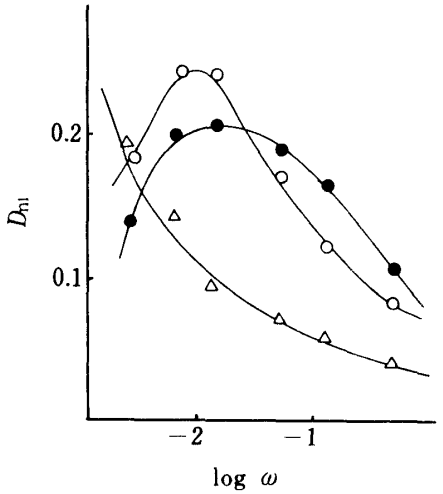

Fig. 9. The Appearance of Maximum D_{nl} Values with Addition of Solid Raw Materials

Symbols: CS 10% (○), BW 10% (●), SA 20% (△).

Comparison of the Oscillation Method and the Continuous Shear Method

In order to understand the rheological properties of such complicated materials as the semisolids used here, the application of other methods and comparison of the results may be useful. Thus, the continuous shear method with a Ferranti-Shirley cone-and-plate viscometer (F.S.) was applied and the results were compared with those of the dynamic methods.

Here, the following relation was assumed for convenience of comparison between the values, y, of the parameters obtained by F.S., such as SYV, η_{120}, or η_{625}, and G' or η'.

$$y = (G' \text{ or } \eta')^{\alpha}$$

The results are summarized in Table II. The correlation coefficients (r) are rather high, even though the results appeared visually to be somewhat scattered about the best straight

Table II. The Relation between the Viscoelastic Parameters (x) and Other Rheological Parameters (y) obtained by F.S.

y	G' (dyn/cm²)			η' (P)		
	α	b	r	α	b	r
SYV (dyn/cm²)	0.57	2.07	0.834	0.64	1.48	0.874
η_{120} (P)	0.47	0.17	0.738	0.51	−0.25	0.734
η_{625} (P)	0.45	−0.44	0.807	0.37	−0.41	0.799

G', η; obtained at $\omega=0.47$ (rad/s).
The relationship between y and x was assumed to be $\log y=\alpha \log x+b$, and α, b, and the correlation coefficient r were calculated by the least-squares method.

line. The relation between G' and SYV and η_{120} is shown in Fig. 10 as examples.

From Table II, it can be seen that α values deviate from 1 in the sequence $\eta_{625}>\eta_{125}>SYV$. It can be presumed that the physical states at which the rheological parameters were measured become more similar to each other as α approaches 1. Therefore the sequence of α in Table II means that as the shear rate increases, the physical state differs more from that reflected by the dynamic method. This result seems reasonable.

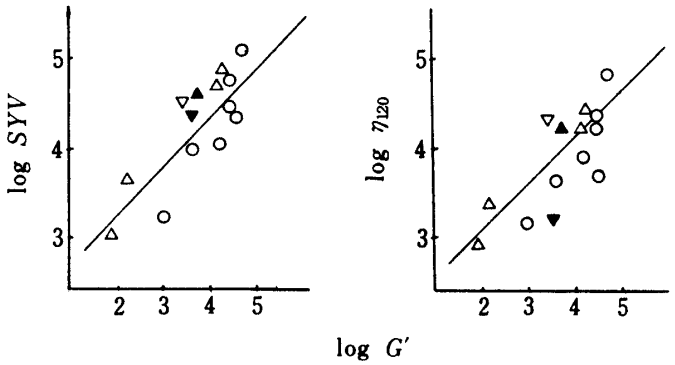

Fig. 10. The Relations between Storage Modulus G' and the Rheological Parameters measured by the Other Method

Symbols: SO (△), MGO (○), LN (▲), HV (▽), WO (▼).

The results shown in Table II also have practical significance because the dynamic properties could be estimated, though roughly, by the F.S. method.

Conclusion

As described above, nonlinear analysis by the oscillation method seems to be easily applicable to most semisolid pharmaceuticals. The ordinal viscoelastic parameters such as G', G'', η', or tan δ can be calculated from the linear part of the stress curve. These parameters seem to account for the major part of σ observed by this method.

On the other hand, the extent of nonlinearity was not negligible for most ointments. The D_{nl} values showed that nonlinearity contributed about 30% to σ at the most, and may correlate with pseudoplastic or thixotropic properties of the materials.

To clarify the physical or pharmaceutical significance of these parameters in further detail, it will be necessary to measure many types of ointments (*e.g.* emulsion, gel, and solid dispersed types) and to compare the results with their other properties.

Some important pharmaceutical properties such as release, crystal growth, physical stability, and so on are intuitively presumed to have a closer correlation with the static state than with the sheared state. We are planning further studies to investigate these relationships.

References and Notes

1) Parts of this work were presented at the 30th Annual Meeting of Kinki Branch, Pharmaceutical Society of Japan, Matsubara, Nov. 1980.

2) E. Shotton and S.S. Davis, *J. Pharm. Pharmacol.*, **20**, 439 (1968); B.W. Barry, *ibid.*, **21**, 533 (1969); *idem*, *J. Colloid. Interface Sci.*, **32**, 551 (1970); B.W. Barry and G.M. Saunders, *ibid.*, **38**, 616 (1972); B.W. Barry and G.M. Eccleston, *J. Texture Stud.*, **4**, 53 (1973); G.M. Eccleston, *J. Pharm. Pharmacol.*, **29**, 157 (1977); G.M. Eccleston, B.W. Barry, and S.S. Davis, *J. Pharm. Sci.*, **62**, 1954 (1973).
3) B.W. Barry and M.C. Meyer, *J. Pharm. Sci.*, **62**, 1349 (1973); B.W. Barry, *J. Pharm. Pharmacol.*, **25**, 131 (1973); B.W. Barry and A.J. Grace, *J. Pharm. Sci.*, **61**, 335 (1972); M.L. DeMartine and E.L. Cussler, *ibid.*, **64**, 976 (1975); J.V. Boyd, *J. Soc. Cosmet. Chem.*, **27**, 247 (1976); H. Oishi, M. Takehara, T. Akinaga, and M. Koike, *Yakuzaigaku*, **28**, 26 (1969).
4) B. Idson, *J. Pharm. Sci.*, **64**, 901 (1975); B.W. Barry and A.J. Grace, *J. Pharm. Pharmacol.*, **22**, 147s (1970).
5) B.W. Barry and B. Warburton, *J. Soc. Cosmet. Chem.*, **19**, 725 (1968).
6) *a*) B.W. Barry and G.M. Eccleston, *J. Pharm. Pharmacol.*, **25**, 244 (1973); *b*) S.S. Davis, *J. Pharm. Sci.*, **60**, 1351 (1971); *c*) *Idem*, *ibid.*, **60**, 1356 (1971).
7) B.W. Barry and E. Shotton, *J. Pharm. Pharmacol.*, **19**, 121s (1967).
8) S. Onogi, T. Masuda, and M. Matsumoto, *Trans. Soc. Rheol.*, **14**, 275 (1970); H. Komatsu, T. Mitsui, and S. Onogi, *ibid.*, **17**, 351 (1973).
9) H. Markovitz, *J. Appl. Phys.*, **23**, 1070 (1952).
10) Vaseline, Penreco USA; lanolin, Takasago Koryo Co., Ltd., Japan; beeswax, Miki Chem. Co., Ltd., Japan; soybean oil, Honen Oil Co., Ltd., Japan; Macrogol 400 and 4000, Nihon Soda Co., Ltd., Japan; cholesterol, Katayama Chemical Co., Ltd., Japan; stearyl alcohol, Kao Soap Co., Ltd., Japan.
11) N.L. Henderson, P.M. Meer, and H.B. Kostenbauder, *J. Pharm. Sci.*, **50**, 788 (1961); J.C. Boylan, *ibid.*, **55**, 710 (1966).
12) T. Kotaka and H. Watanabe, *Nippon Rheology Gakkaishi*, **10**, 24 (1982).
13) M. Reiner, "Deformation, Strain and Flow: An Elementary Introduction to Rheology," H.K. Lewis & Co. Ltd., London, 1960, pp. 236—257.